INSTITUTE OF PHYSICS PUBLISHING JOURNAL OF PHYSICS: CONDENSED MATTER

J. Phys.: Condens. Matter **15** (2003) S31–S45 PII: S0953-8984(03)55828-3

Domains in membranes and vesicles

Reinhard Lipowsky[1] **and Rumiana Dimova**[2]

Max-Planck-Institute of Colloids and Interfaces, 14424 Potsdam, Germany

Received 8 November 2002
Published 16 December 2002
Online at stacks.iop.org/JPhysCM/15/S31

Abstract

Biomimetic membranes such as lipid bilayers with several molecular components exhibit intramembrane domains. These domains are formed after the membranes are quenched into a two-phase coexistence region. Solid domains tend to form facets or cylindrical segments whereas liquid domains tend to form spherical buds. In the latter case, one can distinguish three tension regimes; budding always occurs in the low tension regime for which we present preliminary experimental results for vesicle membranes composed of phospholipid, sphingomyelin and cholesterol. A multicomponent vesicle which adheres to a substrate surface consists of a bound and an unbound membrane segment which differ in their compositions. This shift in composition can induce domains within the bound segment. Such domains are also formed when membranes adhere via sticker molecules and can be driven (i) by the interplay of sticker adhesion and shape fluctuations and (ii) by the competition between sticker and repeller molecules.

Glossary: list of symbols

α, β	two types of membrane phase
A, B	two types of membrane molecule
$\mathcal{A}$	surface area
$\mathcal{A}_\alpha$, $\mathcal{A}_\beta$	surface area of α and β phase
χ_α, χ_β	area fraction of α and β phase
ΔE	activation energy
ΔP	osmotic pressure difference
ΔU	difference in interaction energies across domain boundary
κ	bending rigidity
κ_α	bending rigidity of α domain
λ	line tension of domain boundary
ℓ_{mo}	lateral size of lipid molecule

[1] http://www.mpikg-golm.mpg.de/lipowsky/
[2] http://www.mpikg-golm.mpg.de/th/people/dimova/

L	domain size of single β domain defined via area $\mathcal{A}_\beta = \pi L^2$
L_c	characteristic domain size at which flat domain becomes unstable
L_*	domain size at which flat domain coexists with spherical bud
M	mean curvature of membrane surface
M_{sp}	preferred or spontaneous curvature
$M_{sp,\alpha}$	spontaneous curvature of α domain
$N_{\rm A}$, $N_{\rm B}$	number of A and B molecules
$N_{\rm fac}$	number of facets on vesicle corresponding to rigid solid domains
Ω_c	shape function for domain size L_c
Ω_*	shape function for domain size L_*
$\rho_{\rm ex}$	particle number density in exterior compartment
$R_{\rm ve}$	vesicle size as defined by the surface area
Σ	membrane tension
T	temperature (in energy units)
$U\ cis$	interaction between sticker molecules
$U_{\rm AB}$	interaction energy between A and B lipids
v	volume-to-area ratio
$\mathcal{V}$	volume of vesicle
$\mathcal{V}_{sp}$	volume of spherical shape bounded by the same area
w	reduced and dimensionless adhesion energy per unit area
W	adhesion energy per unit area
ξ	invagination length for domain-induced budding
ξ_Σ	crossover scale arising from the membrane tension Σ
X	mole fraction of A molecules in two-component membrane

1. Introduction

The membranes considered here are bimolecular layers of amphiphilic molecules which form in aqueous solution. These bilayers are very thin with a thickness of a few nanometres but have a large lateral extension up to tens of micrometres. We will focus on bilayers with several components such as phospholipids, cholesterol and anchored macromolecules. These bilayer membranes represent simple model systems for biological membranes which typically contain hundreds of different components [1].

Since multicomponent bilayers are mesoscopic two-dimensional systems, they can exhibit several phases and phase coexistence regions in close analogy with macroscopic three-dimensional systems. If the membrane composition belongs to a coexistence region, one will find different types of membrane domain, i.e., laterally extended regions or zones within the membrane which differ in composition from their surroundings [2].

In the context of biomembranes, textbooks on molecular cell biology such as [3–6] typically discuss the formation of membrane domains which arise from the aggregation of proteins such as clathrin [7] but ignore the possibility that domain formation may also be driven by lipid segregation. The latter process has found renewed interest in the context of 'rafts' which are membrane domains containing phospholipids, sphingomyelin and cholesterol [2, 8–10]. 'Rafts' in biomembranes are difficult to detect experimentally, however, and the evidence for their existence is still rather indirect and controversial. In contrast, for lipid bilayers, it is now possible to obtain direct images of domains in large vesicles using advanced methods of optical microscopy [11, 12].

In this article, the formation and morphology of membrane domains will be discussed from the 'liquid matter' point of view which emphasizes the cooperative behaviour of many molecules. Therefore, we will simplify the terminology for these molecules and use the term 'lipid' as a generic name for phospholipids, glycolipids, sphingomyelin and cholesterol. Likewise, the terms 'sticker' and 'repeller' denote macromolecules which are anchored in the membrane and which are adhesive and nonadhesive, respectively.

We will start from phase diagrams for lipid bilayers which exhibit liquid–solid and liquid–liquid coexistence regions. For such bilayer membranes in water, the terms 'liquid phase' and 'fluid phase' have the same meaning since these membranes cannot exhibit a dilute, vapour-like phase. In addition, we will use the term 'solid membrane' in the sense that the molecules have a fixed lateral connectivity and a nonzero shear modulus.

The simplest procedure to create intramembrane domains is to quench the multicomponent membrane into a coexistence region via a change in temperature or membrane composition. The morphology of the resulting domains depends on their thermodynamic phase. As discussed below, solid domains tend to form facets or cylindrical segments whereas fluid domains tend to form spherical buds.

This article is organized as follows. First, section 2 describes phase diagrams for lipid mixtures and explains the distinction between solid and fluid membranes. We then focus on giant vesicles since they provide rather convenient model systems for which one has several control parameters, see section 3. The main part of this article is about the morphology of multi-domain vesicles as discussed in section 4 and about domain formation induced by membrane adhesion, see section 5. There are several distinct mechanisms for adhesion-induced membrane domains; a particularly simple one is provided by the change in membrane composition arising from the interaction with the substrate surface. At the end, we give a brief outlook and propose fusion of aspirated vesicles as an alternative method to create vesicles with multi-domain patchworks.

Even though this article is basically a review of previous theoretical work from our group, it contains several original pieces: the prediction that solid domains in a fluid matrix tend to form cylindrical segments, see section 4.1; the identification of three different tension regimes for budding of fluid domains and preliminary experimental results for the low-tension regime, see section 4.2, and theoretical results for adhering vesicles in the limit of strong adhesion which leads to changes in vesicle volume and to shifts in the membrane composition, see section 5.

2. Domain formation via phase separation

2.1. Phase diagrams

For many two-component membranes, the phase diagram has been determined experimentally using a variety of experimental methods. If the membranes contain two phospholipids, their phase diagram typically exhibits a solid–liquid coexistence region as shown in figure 1(a). Similar studies have also been performed for binary mixtures of one phospholipid and cholesterol. For DPPC and cholesterol, the corresponding phase diagram exhibits three coexistence regions as shown in figure 1(b) [13]. In addition, ternary phase diagrams have been determined for a few three-component membranes containing two phospholipids and cholesterol [14, 15]. The phase diagram determined in [14] is schematically shown in figure 1(c).

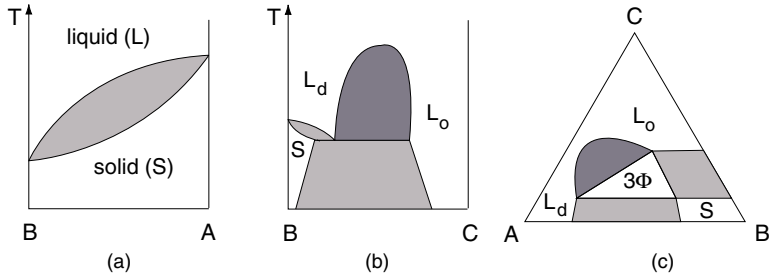

Figure 1. Schematic phase diagrams as a function of membrane composition and temperature T: (a) binary mixture of two phospholipids A and B, (b) binary mixture of phospholipid B and cholesterol C and (c) ternary mixture of A, B and C at room temperature. Solid phases are denoted by S, liquid (or fluid) phases by L; the subscripts o and d stand for 'ordered' and 'disordered', respectively. Two-phase coexistence regions between a solid and a liquid phase are light grey; the corresponding regions between two liquid phases are dark grey. The three-phase coexistence region in (c) is denoted by 3Φ.

2.2. Solid versus fluid membranes

At this point, it is useful to recall the basic distinction between solid and fluid membranes. Within a solid phase, the membrane molecules have a fixed connectivity and the membrane resembles a thin plate. According to classical elasticity theory, such a plate can undergo three types of elastic deformation: stretching, shearing and bending [16, 17]. If such a solid plate is deformed into a spherical segment characterized by a nonzero Gaussian curvature, it has to be stretched locally in order to satisfy the constraint of fixed connectivity. This can be done with a sheet of rubber which is relatively easy to stretch but is essentially impossible for a sheet of paper which is (almost) incompressible. Thus, a solid membrane, which is (almost) incompressible (or unstretchable), can exhibit only one-dimensional bends with vanishing Gaussian curvature corresponding to cylindrical membrane segments. This incompressible limit is appropriate for lipid bilayers since these membranes rupture when their area is increased by a few per cent.

In contrast to solid membranes, liquid or fluid membranes have a vanishing shear modulus and any shear deformation relaxes by flow within the membrane. Thus, they can exhibit two-dimensional bends and form spherical segments with nonvanishing Gaussian curvature. The corresponding bending energy is governed by two elastic parameters, the bending rigidity κ and the spontaneous curvature M_{sp}.

The bending rigidity of lipid bilayers in the fluid phase is of the order of 10^{-19} J. The spontaneous curvature depends on the molecular structure of the bilayer and on its interactions with its environment. It can be controlled, to some extent, by the concentration of anchored polymers and dispersed particles, see, e.g., [2, 18–20]. If the exchange of molecules (or rate of flip–flops) between the two monolayers is slow, one has an additional contribution to the spontaneous curvature arising from the area difference of the two monolayers [21].

2.3. Quench into coexistence region

Now, if one changes the temperature or composition in such a way that the membrane is quenched into a coexistence region, its composition will become heterogeneous and the membrane will undergo lateral phase separation which should lead to the formation of intramembrane domains as observed in [11, 12]. As in other two-dimensional systems, these domains should be formed by nucleation or spinodal decomposition.

For a 'shallow' quench which leads to a state within the coexistence region but close to the original one-phase region, one has to overcome a nucleation barrier with an activation energy ΔE which is large compared to T (here and below, the temperature is measured in energy units, i.e., the Boltzmann factor has been absorbed into the symbol T). After a nucleation time $\sim \exp(\Delta E/T)$, the first domain appears which will then grow by diffusion-limited aggregation within the membrane. For a 'deep' quench, on the other hand, there is no such barrier and one expects the formation of many small domains. The largest domains are expected to grow by the 'evaporation' of smaller ones (Lifshitz–Slyozov mechanism) and by the coalescence with other domains.

Since bilayer membranes consist of two monolayers, one could, in principle, have monolayer domains, which extend only across a single monolayer, or bilayer domains, which extend across both monolayers. Monolayer domains will usually have a nonzero spontaneous curvature M_{sp} whereas bilayer domains should be typically characterized by $M_{sp} = 0$ [22]. This distinction was addressed experimentally in [11] for the solid–liquid coexistence of DLPC/DPPC membranes. In this case, all domains were found to be bilayer domains.

This can be understood from the theoretical point of view if one considers the 'buried' interface between the two monolayers of a membrane domain. If this domain extends across both monolayers, the packing density of the hydrocarbon groups should be rather similar on both sides of this interface. For a monolayer domain, on the other hand, one monolayer would be in the solid phase, the other in the fluid phase, and the hydrocarbon density would change across this interface. Thus, the tension of the 'buried' interface should be larger for a monolayer domain which favours the bilayer domain.

2.4. Morphologies of flat domains

Let us assume, for a moment, that we have a multi-domain bilayer which is essentially flat. One might then expect to find domains which are similar to those observed for lipid monolayers at the air–water interface. The simplest case is provided by the coexistence of two fluid phases for which the line tension of the domain boundary is isotropic and the domains have a circular equilbrium shape as observed for many monolayer systems. For solid-like domains, on the other hand, the line tension becomes anisotropic, and the domains are no longer circular. In fact, for lipid monolayers, one sometimes finds peculiar domain shapes which may be governed by long-ranged dipolar interactions [23, 24]. For bilayer membranes in water, dipolar forces are expected to be less important. Thus, we will assume here that the domain shape in a flat bilayer membrane is primarily determined by the line tension of the domain boundary.

2.5. Line tension of domain boundaries

In order to estimate the line tension λ of the domain boundary, we may consider two adjacent domains consisting of two different types of lipid, say A and B. A simple estimate is then given by $\lambda \simeq \Delta U/\ell_{mo}$ with the energy difference $\Delta U \equiv [\frac{1}{2}(U_{AA}+U_{BB})-U_{\rm AB}]$ where $\ell_{mo} \simeq 0.8$ nm is the lateral size of the lipid molecules and U_{AA}, U_{BB} and $U_{\rm AB}$ are the various pair interactions. If one takes these pair interactions to be of the order of T, one obtains $\lambda \simeq 10^{-11}$ N.

So far, there are no experimental data for the line tension in lipid bilayers but there are some measurements in lipid monolayers at the air–water interface. For a mixture of a phospholipid (DMPC) and 30% cholesterol, the corresponding line tension has been measured to be about 2×10^{-12} N at zero lateral pressure [25]. Furthermore, an increase in the lateral pressure leads to a decrease of λ by two orders of magnitude which indicates the vicinity of a critical point in the monolayer at the air–water interface. In order to use these measurements for an estimate

of the line tension in lipid bilayers, one would have to know what value of the lateral pressure leads to the same lipid density as found in the bilayer membrane.

Another mechanism, which can lead to anomalously small line tensions, applies to mixed membranes with more than two components if some of these components are strongly adsorbed at the domain boundaries. Such a situation represents the two-dimensional analogue of a microemulsion in three dimensions.

3. Giant vesicles as model systems

Membranes are typically curved and the coupling between this curvature and the membrane composition has a strong influence on the membrane morphology. This coupling can be studied in giant vesicles which provide convenient model systems. Indeed, the shape of these vesicles, which can be directly observed in the light microscope, is governed by a few parameters, some of which can be varied in a systematic way. These parameters are explained in the following subsections.

3.1. Volume-to-area ratio

Lipid membranes in water have two important properties. Since the membrane molecules are highly insoluble in water, the total area $\mathcal{A}$ of the membrane is conserved (at constant temperature and constant osmotic conditions). In addition, these membranes are permeable to water but highly impermeable to ions, macromolecules and nanoparticles which implies that the vesicle adapts its volume in such a way that the interior and exterior compartments are osmotically balanced. Thus, the vesicle volume $\mathcal{V}$ is also conserved for fixed number of osmotically active particles in the vesicle interior and for fixed number density of such particles in the exterior compartment (as long as the number densities of the osmotically active particles are large compared to $\kappa/T\mathcal{V}$).

Therefore, the most important quantity which determines the shape of giant vesicles is the volume-to-area ratio as defined by

$$v \equiv \mathcal{V}/\mathcal{V}_{sp} \qquad \text{where } \mathcal{V}_{sp} \equiv \frac{4\pi}{3}(\mathcal{A}/4\pi)^{3/2} \tag{1}$$

is the volume of a sphere with area $\mathcal{A}$. This geometric quantity satisfies $0 \leqslant v \leqslant 1$ and represents a control parameter which can be varied by changes in temperature and osmotic conditions.

Since the thermal expansivity of lipid bilayers is larger than the expansivity of water, the volume-to-area ratio v decreases with increasing temperature. Changes in the osmotic conditions lead to inflation or deflation and, thus, to an increase or decrease of v, respectively.

3.2. Tense vesicles and droplet limit

A giant vesicle with volume-to-area ratio $v < 1$, which is bounded by a fluid membrane and does not experience external forces, is essentially tensionless. More precisely, the tension within the vesicle membrane is of the order of $\kappa/R_{\rm ve}^2$ where κ and $R_{\rm ve}$ are the bending rigidity of the membrane and the vesicle radius as before. For a lipid bilayer with $\kappa \simeq 10^{-19}$ J and a vesicle radius $R_{\rm ve} \simeq 10\ \mu$m, one obtains $\kappa/R_{\rm ve}^2 \simeq 10^{-6}$ mJ m^{-2} which is indeed a rather small tension. However, there are several additional mechanisms which can induce a tension $\Sigma \gg \kappa/R_{\rm ve}^2$ within the membrane:

(i) inflation by the osmotic pressure;

(ii) adhesion to a substrate surface and
(iii) formation of solid domains.

In general, Σ can grow up to the tension of rupture which is of the order of a few mJ m^{-2}.

The membrane tension defines the crossover length $\xi_\Sigma \equiv (4\kappa/\Sigma)^{1/2}$: on length scales which are small compared to ξ_Σ, the shape fluctuations of the membrane are still governed by the bending rigidity κ; on length scales which are large compared to ξ_Σ, on the other hand, the shape fluctuations are governed by this tension. If one observes the vesicle in this latter regime, the vesicle behaves like a liquid droplet with adjustable volume.

3.3. Membrane composition and area fraction

Now, consider a multicomponent membrane with a composition corresponding to one of its coexistence regions, compare figure 1. For simplicity, we will focus on the coexistence of *two* phases, denoted again by α and β.

If the vesicle membrane undergoes complete phase separation, it will consist of one large α domain and one large β domain. The corresponding areas $\mathcal{A}_\alpha$ and $\mathcal{A}_\beta$ define the area fractions

$$\chi_\alpha \equiv \mathcal{A}_\alpha/\mathcal{A} \qquad \text{and} \qquad \chi_\beta \equiv \mathcal{A}_\beta/\mathcal{A} = 1 - \chi_\alpha \tag{2}$$

where the total vesicle area is given by $\mathcal{A} = \mathcal{A}_\alpha + \mathcal{A}_\beta$. These area fractions can be expressed in terms of the mole fractions of the coexisting phases and in terms of the specific molecular areas of the lipids in these different phases.

4. Morphology of multi-domain vesicles

Now, consider a vesicle with a membrane which contains two types of phase domain, α and β. If both domains were solid, the membrane would have to make some sharp edges or to break up, a situation which we will not consider here. Therefore, one type of domain, say β, is always taken to be fluid. Furthermore, we will implicitly assume that spatial variations of the membrane composition are limited to the domain boundaries and that the width of these boundaries is much smaller than the size of the domains. This is sometimes called the strong-segregation limit of phase separation.

4.1. Solid domains in fluid membranes

For a typical binary system with a phase diagram as shown in figure 1(a), a quench into the two-phase coexistence region will produce solid domains in a fluid membrane. As mentioned, these segments of solid membrane can be viewed as thin plates. One may then consider two simple but instructive cases:

(i) the limit of large bending rigidity and
(ii) the limit of small area compressibility.

In these limits, the curvature of the vesicle (i) truncates the phase separation process and (ii) determines the morphology of the intramembrane domains.

Vesicles with facets. If the solid α domains are rather rigid, they will form planar facets within the fluid β phase. Such vesicles have been observed by several groups but, as far as we know, no systematic studies have been published.

As the vesicle develops facets, its membrane will develop a tension since a facetted vesicle can accommodate less volume than a spherical one. Two possibilities arise:

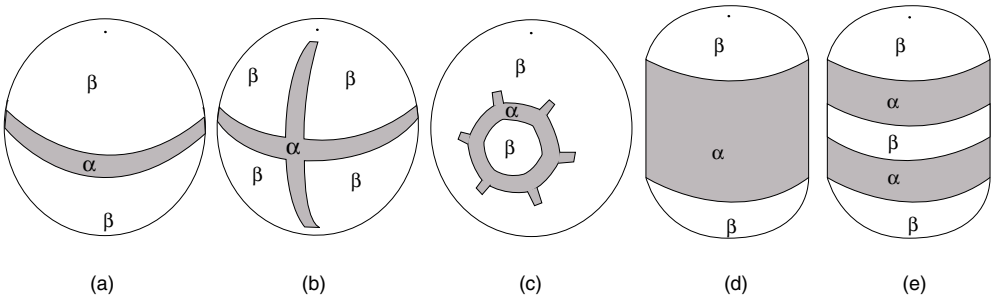

Figure 2. Vesicles with stripe domains containing solid α and fluid β domains. All solid α domains (grey) have the shape of cylindrical segments with vanishing Gaussian curvature. If the vesicle is inflated and essentially spherical, the solid phase can form narrow stripes as in (a)–(c). If the vesicle is deflated and prolate, the solid phase can form barrels as in (d) and (e).

(i) the domains will coalesce and grow until the vesicle ruptures or

(ii) the phase separation process will be stopped or 'frustrated' by the geometric constraints.

If one compares the decrease in the free energy of the domain boundaries arising from the coarsening process with the work required to increase the membrane tension beyond the tension of rupture, one finds that case (ii) should be typical for giant vesicles as discussed here.

In this latter case, the vesicle will attain the shape of a β sphere with a certain number $N_{\rm fac}$ of α facets. If these facets are all of comparable size, this number behaves as

$$N_{\rm fac} \approx \frac{3}{2}\chi_\alpha^2 \frac{1}{1-v} \qquad \text{for small } 1-v \tag{3}$$

where the volume-to-area ratio v and the area fraction χ_α have been defined in (1) and (2), respectively. For sufficiently small v, on the other hand, the phase separation process can lead to vesicles with a single facet; the corresponding vesicle shapes will resemble those found for the weak adhesion to planar substrates, see, e.g., [26].

Vesicles with stripe domains. If the solid α domains are less rigid, they may be bent into cylindrical segments characterized by vanishing Gaussian curvature. If one starts from a closed vesicle which is essentially spherical, the solid domains can form narrow stripes as shown in figures 2(a)–(c). These morphologies are reminiscent of those found experimentally in [11]. Note that more complex networks of stripes are possible; thus, one could have a 'soccer vesicle' where the α domains form the edges of 12 pentagons and 20 hexagons. If the vesicle has a prolate shape, one might end up with the barrel-type morphologies shown in figures 2(d) and (e).

In principle, it would not be difficult to calculate the equilibrium states for such vesicles in a systematic way. These shapes depend on the bending rigidities of the two membrane phases, on their spontaneous curvatures and on the line tension of the domain boundaries. If one decreases this line tension, the number of stripes should increase and the width of the stripes should decrease. Such an effect has been observed in [11] after the addition of cholesterol to the membrane. In practice, the freezing process may lead to various types of defect and the resulting morphologies will then be less ordered than those shown in figure 2.

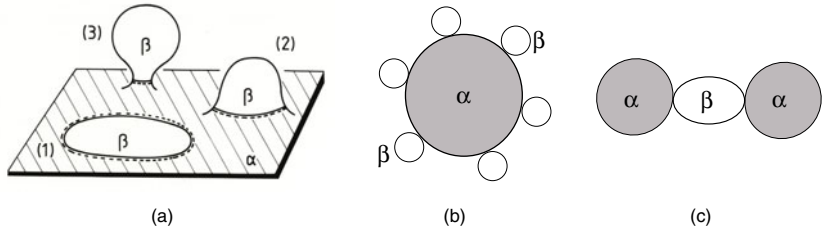

Figure 3. (a) Domain-induced budding of a membrane segment must occur as soon as the size of the β domain exceeds a certain threshold value provided the tension within the membrane is sufficiently small; (b) a large α vesicle decorated with many β buds which may arise via phase separation as studied in [29] and (c) vesicle with a β bud sandwiched between two α buds.

4.2. Fluid domains in fluid membranes

Now, let us consider a mixture which exhibits a coexistence region of two fluid phases as shown in figure 1(b) or (c). If we quench the system into this two-phase coexistence region, we obtain two different types of fluid domain, α and β. In this case, the domains have a tendency to form buds as indicated in figure 3 [22, 27–29].

Domain-induced budding. First, consider a single β domain of area $\mathcal{A}_\beta$ surrounded by α phase. If the domain is essentially flat and has a linear size $L \equiv (\mathcal{A}/\pi)^{1/2}$, the excess free energy associated with its boundary line is $\sim\lambda L$ which grows linearly with L. If we transform the domain into a spherical bud connected to the α phase by a small neck, we get rid of this line energy but must pay some bending energy. For vanishing spontaneous curvature, the latter energy is, however, independent of the domain size which implies that the flat domain must bud as soon as it has reached a certain characteristic size L_c. A nonzero spontaneous curvature breaks the symmetry between the two sides of the bilayer but acts to make the budding process even more favourable.

If one ignores the curvature of the surrounding α membrane, the characteristic domain size L_c of the β domain with bending rigidity κ is given by [22, 27]

$$L_c = L_c(\xi, M_{sp}) = \xi\Omega_c(\xi|M_{sp}|) \tag{4}$$

which depends on the spontaneous mean curvature M_{sp} of the β domain and on the invagination length $\xi \equiv \kappa/\lambda$. The shape function $\Omega_c(x)$ decreases monotonically with increasing $x \equiv \xi M_{sp}$. Therefore, one has $L_c(\xi, M_{sp}) \leqslant \xi\Omega_c(0)$. The spherical cap model studied in [22, 27], which ignores the precise shape of the neck region, leads to $\Omega_c(0) = 8$. Using these relations, the characteristic domain size L_c has been estimated to be of the order of 80–800 nm for lipid bilayers [2, 22]. Within the spherical cap model, one can also calculate the domain size $L = L_*$ for which the flat domain and the spherical bud have the same free energy; the latter length is given by $L_* = \xi\Omega_*(\xi|M_{sp}|)$ with $\Omega_*(0) = 4$.

Neck condition. A vesicle which consists of two fluid domains α and β often attains a limit shape in which the β domain forms a complete bud, i.e., a spherical bud which is connected to the mother vesicle by an infinitesimal neck. In the spherical cap model, the boundary between the two domains is assumed to be located within the neck since it then has the smallest length and, thus, the smallest energy. This assumption is confirmed by a systematic minimization for two-domain vesicles [28].

Adjacent to the neck region, the mean curvature M of the budded β domain and the mean curvature M_α of the mother vesicle satisfy the condition [28]

$$\kappa(M - M_{sp}) + \kappa_\alpha(M_\alpha - M_{sp,\alpha}) = \lambda/2 \tag{5}$$

where the bending rigidities, κ and κ_α, and the spontaneous mean curvatures, M_{sp} and $M_{sp,\alpha}$, of the β and α domains will usually be different. If the second term on the left-hand side of (5) is small, this relation leads to the characteristic domain size $L_c = 2/M \approx 4\xi/(1 + 2\xi M_{sp})$ which is equivalent to (4) with $\Omega_c(0) = 4$. In principle, the neck condition (5) could be used to determine the line tension λ from a measurement of the mean curvatures M^β and M^α provided the spontaneous curvatures are sufficiently small and can be ignored.

Volume constraint and membrane tension. The balance between the line and bending energies, as described above, is appropriate as long as the membrane does not experience additional constraints. For vesicles, one has the constraints on membrane area and vesicle volume which tend to suppress the formation of buds [28]. This can be understood within the spherical cap model if one considers a single β domain surrounded by α membrane which is subject to a tension as discussed in [22]. One then finds three different regimes for the membrane tension Σ (which we take to have the opposite sign from the one used in [22]). These three tension regimes are separated by the characteristic tensions $\Sigma_1 \equiv \kappa/32\xi^2 = \lambda^2/32\kappa$ and $\Sigma_2 \equiv \lambda^2/8\kappa$ which depend on the bending rigidity κ of the β domain and on the line tension λ of the domain boundary.

For $0 < \Sigma \leqslant \Sigma_1$, one has basically the same situation as for the tensionless case: the flat domain with $M = 0$ becomes unstable at the characteristic size $L_c = L_c(\Sigma)$ which increases with Σ and grows up to $L_c = 16\xi$ for $\Sigma = \Sigma_1$. If the tension satisfies $\Sigma_1 < \Sigma \leqslant \Sigma_2$, the flat domain stays metastable for all values of the domain size L but there is an intermediate range of L-values for which the free energy of the bud state with mean curvature $M = 2/L$ is smaller than the free energy of the flat domain state with $M = 0$. In the latter case, the domain may transform into a bud if it overcomes the activation barrier which separates these two states. Finally, for sufficiently large tensions $\Sigma > \Sigma_2$, the flat state has the lowest free energy for all values of L.

The characteristic tensions Σ_1 and Σ_2 are proportional to $\Sigma_{sc} \equiv \kappa/\xi^2 = \lambda^2/\kappa$ which defines the basic tension scale for this problem. For lipid bilayers with $\kappa = 10^{-19}$ J and $\lambda = 10^{-11}$ N, one has $\Sigma_{sc} = 1$ mJ m^{-2} which is somewhat smaller than the tension of rupture. This implies that all three tension regimes should be accessible to experimental studies.

Experiments. Very recently, fluid domains in fluid membranes have been directly observed by optical microscopy for three-component membranes containing phospholipid (DOPC), cholesterol and sphingomyelin [12]. So far, only one composition characterized by identical mole fractions for all three components has been studied. Furthermore, the vesicles observed in [12] were presumably inflated and, thus, could not undergo domain-induced budding. In contrast, for deflated vesicles with the same membrane composition, we observe a strong tendency for budding as shown in figure 4. What remains to be done is to use fluorescent probes for these deflated vesicles in order to visualize their intramembrane domains. In addition, the different domains will differ in their rheological properties which can be determined by the experimental methods described in [30].

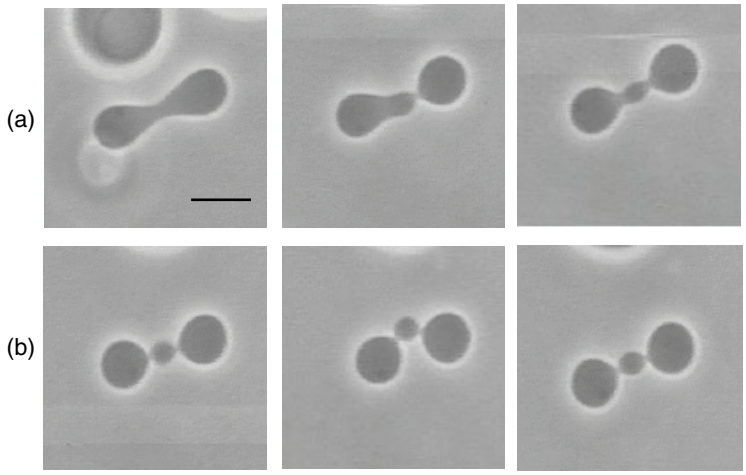

Figure 4. Optical micrographs of a three-component vesicle which contains the same mole fractions of phospholipid (DOPC), cholesterol and sphingomyelin: (a) shape sequence induced by heating and (b) dumbbell fluctuations at constant temperature (25 °C). Cooling leads to a shape sequence which corresponds to the inverse of the sequence shown in (a). We believe that the underlying domain structure corresponds to figure 3(c). The bar represents 10 μm.

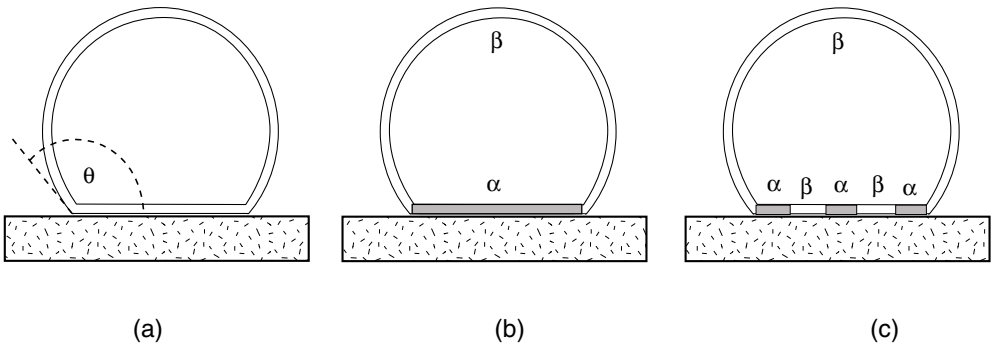

Figure 5. Strong adhesion of vesicles to a substrate surface: (a) the vesicle resembles a droplet with effective contact angle θ and adjustable volume; (b), (c) the substrate recruits the A lipids to the contact area and, thus, induces phase separation into an A-rich phase α and an A-poor phase β. If α is a solid phase, the membrane composition within the contact area in (b) and (c) corresponds to the one-phase region S and to the two-phase region in the phase diagram of figure 1(a), and one has adhesion-induced solidification.

5. Domain formation via adhesion

5.1. Weak versus strong adhesion

As mentioned, vesicles which experience a relatively large tension behave like droplets with an adjustable volume. Therefore, if such a vesicle adheres to a substrate surface, it will attain the shape of a spherical cap as shown in figure 5(a). In contrast to a liquid droplet, the volume of this cap is not fixed, however, but is determined by the balance between the adhesion and the osmotic pressure arising from dispersed 'particles' which cannot permeate the membrane.

As an example, consider a vesicle of radius $R_{\rm ve} = (\mathcal{A}/4\pi)^{1/2}$ with volume-to-area ratio $v = 1$ which is osmotically balanced with the exterior 'particle' concentration $\rho_{\rm ex}$. If this

vesicle is attracted to a substrate with adhesion energy W per unit area, the volume-to-area ratio v of the spherical cap depends on the dimensionless adhesion parameter $w \equiv 2|W|/(T R_{\rm ve} \rho_{\rm ex})$ and is given by

$$v \approx 1 - \frac{3}{2}\left(\frac{w}{3}\right)^{2/3} \qquad \text{for small } w \tag{6}$$

and by

$$v \approx \frac{3}{2}\left(\frac{2}{3w}\right)^{1/2} \qquad \text{for large } w. \tag{7}$$

In the derivation of these relations, the finite area compressibility, which can change v by a few per cent, has been ignored.

5.2. Adhesion-induced shift of coexistence line

Now, assume that the membrane of the adhering vesicle contains two lipid components, A and B. In general, these two components will experience different forces arising from the substrate surface. Let us assume, for example, that the membrane contains negatively charged A molecules and electrically neutral B molecules which interact with a positively charged substrate surface. In such a situation, the substrate surface attracts the A molecules strongly by electrostatic forces whereas the B molecules are attracted only weakly by van der Waals forces. For a fluid membrane, the molecules can diffuse laterally and the more strongly attracted component will be recruited to the contact area of the adhering vesicle.

Depending on the topography and the chemical composition of the substrate surface, one may have some kinetic barriers for the lateral diffusion within the contact area. One example for such a barrier is provided by membrane adhesion via stickers and repellers which is briefly discussed further below. On the other hand, if the A and B molecules are comparable in size, and if the substrate surface is smooth and uniform, this kinetic barrier is expected to be small since the bound segment of the adhering vesicle is not in direct contact with the substrate surface but is separated from it by a water layer of one to two nanometres.

The overall composition of the two-component vesicle membrane can be characterized by the mole fraction $X \equiv N_{\rm A}/(N_{\rm A} + N_{\rm B})$ of the A molecules where $N_{\rm A}$ and $N_{\rm B}$ are the total number of A and B molecules, respectively. For the unbound vesicle, two-phase coexistence corresponds to $X_\beta(T) < X < X_\alpha(T)$ with temperature-dependent mole fractions X_β and X_α corresponding to the β and α phases, respectively, compare figure 1. In the following, we will consider vesicles with $X < X_\beta$ which implies that the membranes of the unbound vesicles have uniform composition corresponding to the fluid β phase.

If such a vesicle adheres to a substrate surface which attracts the A molecules more strongly, the bound membrane segment of the vesicle will acquire an A-rich composition characterized by the mole fraction $X' > X$ whereas the unbound membrane segment of the vesicle will acquire an A-poor composition with mole fraction $X'' < X$.

If the mole fraction X' of the bound segment satisfies $X_\alpha(T) < X'$, this segment is in the α phase whereas the unbound segment of the vesicle stays in the β phase. This is the situation shown in figure 5(b). Thus, if the α phase is solid, the adhesion process leads to solidification of the membrane within the contact area. On the other hand, if X' satisfies $X_\beta < X' < X_\alpha$, the bound membrane segment will undergo phase separation into α and β domains as indicated in figure 5(c). During the initial stages of these processes, the total vesicle area may again change if the specific molecular areas of the lipid components are different in the two phases.

5.3. Adhesion via sticker molecules

If only one of the two components, say A, is attracted to the substrate, this component acts as a sticker molecule. It is now useful to distinguish two types of interaction:

(i) *trans* interactions between one such sticker with the substrate surface and
(ii) *cis* interactions between two stickers within the same membrane.

The strength of the latter interactions, which may be repulsive or attractive, will be denoted by U [31].

Adhesion via stickers frequently leads to domain formation within the contact area. Several mechanisms for this process must be distinguished. First, if the *cis* interaction U is attractive, the unbound membrane undergoes phase separation provided the attractive strength U of the *cis* interactions exceed a certain threshold value U_c. This threshold value is significantly reduced if the membrane adheres to another surface [32, 33]. This reduction represents a renormalization of the *cis* interactions by the confined membrane fluctuations.

Secondly, if the *cis* interactions are purely repulsive, phase separation into sticker-rich and sticker-poor domains also occurs if the size of the stickers is larger than the size of the non-adhesive membrane components [32]. This process is driven by an effective line tension which depends on the size of the stickers and arises from the interplay of shape fluctuations and sticker clusters. Likewise, phase separation also occurs, for purely repulsive *cis* interactions, if the rigidity of the stickers is larger than the rigidity of the non-adhesive components [33]. In both cases, the mechanism for domain formation is of purely entropic origin.

Thirdly, membrane adhesion can lead to domain formation if the membrane contains both stickers and repellers. The latter types of molecule are nonadhesive but protrude from the membrane surface and, thus, impose a steric barrier for the adhesion. If all *cis* interactions between the stickers and repellers are purely repulsive, one may integrate over the composition variables and derive an effective potential for the membrane–membrane interactions which has a potential barrier [33, 34]. Such a potential barrier represents an energetic mechanism for domain formation.

In the presence of an effective potential barrier, the adhesion dynamics represents a nucleation process [35]. Thus, in the presence of repellers, adhesion is governed by the nucleation of sticker clusters or islands. The diffusion and coalescence of these clusters leads to the formation of distinct domain patterns at intermediate times [36]. For relatively large barriers arising from long repellers, a single sticker domain is nucleated within the contact area which grows via the condensation of additional stickers. For relatively small barriers, on the other hand, many sticker domains are formed initially. As additional stickers diffuse into this area, they tend to condense at those domains which are close to the contact line. At intermediate times, these sticker domains coalesce and form an outer ringlike domain of stickers which encloses an inner domain of trapped repellers (this represents the previously mentioned example for a kinetic barrier which suppresses lateral diffusion within the contact area). At later times, this domain pattern is inverted and one obtains one large sticker domain which is surrounded by repellers. Very similar patterns have been observed in the immunological synapse between T cells and antigen-presenting cells for which the sticker molecules correspond to MHC peptides [37].

6. Outlook

In this article, we have discussed intramembrane domains in the context of bilayer membranes which contain only a few membrane components. However, similar domains should be present

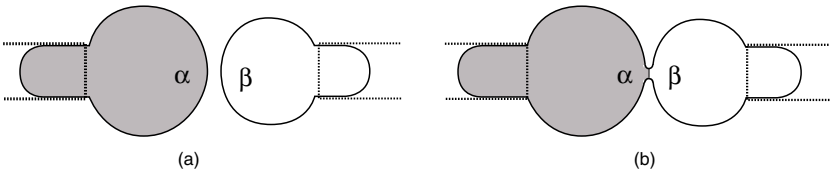

Figure 6. Possible procedure to create membranes with multi-domain patchworks: (a) using micropipettes, two vesicles with different liquid phases α and β are brought into close proximity, and (b) after the two membranes have fused, one obtains a vesicle with two large intramembrane domains.

for biomembranes which are composed of a very large number of different lipids and proteins. As mentioned, it is now believed that biomembranes contain 'rafts' which are membrane domains built up from phospholipids, sphingomyelin and cholesterol [2, 8–10]. Some of these rafts seem to form caveolae which are small buds of the plasma membrane. It is interesting to note that the cartoons which have recently appeared in the biological literature in order to illustrate the formation of caveolae from rafts [38, 39] are rather similar to the process of domain-induced budding as shown in figure 3(a).

Likewise, the immune response of T cells and antigen-presenting cells leads to characteristic domain patterns within the immunological synapse, i.e., within the contact area of these cells [37, 40, 41]. These patterns exhibit a time evolution which is rather similar to the nucleation process discussed at the end of the previous section arising from the interplay between stickers and repellers.

Finally, it is interesting to note that biomembranes frequently change their topology by fission and fusion processes. The latter processes could provide an alternative procedure in order to construct multidomain vesicles as indicated in figure 6. First, one has to prepare two vesicles with different compositions α and β which correspond to two coexisting phases (at a certain temperature). These vesicles are then grabbed by two micropipettes and brought into close proximity as shown in figure 6(a). Finally, the adjacent vesicle membranes fuse which will lead to the two-domain vesicle shown in figure 6(b). In principle, such a procedure could be repeated several times and, thus, could lead to membranes with a multi-domain patchwork.

References

[1] Lipowsky R and Sackmann E (ed) 1995 Structure and dynamics of membranes *Handbook of Biological Physics* vol 1 (Amsterdam: Elsevier)
[2] Lipowsky R 2002 *J. Biol. Phys.* **28** 195
[3] Alberts B *et al* 1994 *Molecular Biology of the Cell* 3rd edn (New York: Garland)
[4] Lodish H *et al* 1995 *Molecular Cell Biology* 3rd edn (New York: Freeman)
[5] Tobin A and Morel R 1997 *Asking about Cells* 1st edn (Fort Worth: Saunders)
[6] Cooper G 1997 *The Cell* (Sunderland: Sinauer)
[7] Schekman R and Orci L 1996 *Science* **271** 1526
[8] Simons K and Ikonen E 1997 *Nature* **387** 569
[9] Jacobson K and Dietrich C 1999 *Trends in Cell Biology* **9** 87
[10] Huttner W and Zimmerberg J 2001 *Curr. Opin. Cell Biol.* **13** 478
[11] Korlach J, Schwille P, Webb W and Feigenson G 1999 *Proc. Natl Acad. Sci. USA* **96** 8461
[12] Dietrich C *et al* 2001 *Biophys. J.* **80** 1417
[13] Bloom M and Mouritsen O G 1995 The structure and dynamics of membranes *Handbook of Biological Physics* vol 1, ed R Lipowsky and E Sackmann (Amsterdam: Elsevier) pp 65–95
[14] Silvius J, del Giudice D and Lafleur M 1996 *Biochemistry* **35** 15198
[15] Feigenson G W and Buboltz J T 2001 *Biophys. J.* **80** 2775
[16] Landau L and Lifschitz E 1991 *Lehrbuch der Theoretischen Physik. VII. Elastizitätstheorie* (Berlin: Akademie)

[17] Komura S and Lipowsky R 1992 *J. Physique* II **2** 1563
[18] Lipowsky R, Döbereiner H G, Hiergeist C and Indrani V 1998 *Physica* A **249** 536
[19] Lipowsky R 1999 *Statistical Mechanics of Biocomplexity (Springer Lecture Notes in Physics)* ed D Reguera, J M Rubi and J M B Vilar (Berlin: Springer) pp 1–23
[20] Dimova R, Döbereiner H G and Lipowsky R 2002 *Biophys. J.* **82** 506a
[21] Miao L, Seifert U, Wortis M and Döbereiner H-G 1994 *Phys. Rev.* E **49** 5389
[22] Lipowsky R 1992 *J. Physique* II **2** 1825
[23] Keller D, McConnell H and Moy V 1986 *J. Phys. Chem.* **90** 2311
[24] Andelman D, Brochard F and Joanny J-F 1987 *J. Chem. Phys.* **86** 3673
[25] Benvegnu D and McConnell H 1992 *J. Phys. Chem.* **96** 6820
[26] Kraus M, Seifert U and Lipowsky R 1995 *Europhys. Lett.* **32** 431
[27] Lipowsky R 1993 *Biophys. J.* **64** 1133
[28] Jülicher F and Lipowsky R 1993 *Phys. Rev. Lett.* **70** 2964
Jülicher F and Lipowsky R 1996 *Phys. Rev.* E **53** 2670
[29] Kumar S, Gompper G and Lipowsky R 2001 *Phys. Rev. Lett.* **86** 3911
[30] Dimova R, Pouligny B and Dietrich C 2000 *Biophys. J.* **79** 340
[31] Lipowsky R 1996 *Phys. Rev. Lett.* **77** 1652
[32] Weikl T, Netz R and Lipowsky R 2000 *Phys. Rev.* E **62** R45
[33] Weikl T and Lipowsky R 2001 *Phys. Rev.* E **64** 011903/1
[34] Weikl T, Andelman D, Komura S and Lipowsky R 2002 *Eur. Phys. J.* E **8** 59
[35] Lipowsky R 1994 *J. Physique* II **4** 1755
Ammann A and Lipowsky R 1996 *J. Physique* **6** 255
[36] Weikl T, Groves J and Lipowsky R 2002 *Europhys. Lett.* **59** 916
[37] Grakoui A *et al* 1999 *Science* **285** 221
[38] Galbiati F, Razani B and Lisanti M P 2001 *Cell* **106** 403
[39] Shin J-S and Abraham S 2001 *Science* **293** 1447
[40] Monks C *et al* 1998 *Nature* **395** 82
[41] Davis D *et al* 1999 *Proc. Natl Acad. Sci. USA* **96** 15062